A two-phase model for chemo-damage induced anisotropy in concrete

Claudia Comi[1], Umberto Perego[2]
Department of Structural Engineering, Politecnico di Milano, Italy
[1] *E-mail: claudia.comi@polimi.it*
[2] *E-mail: umberto.perego@polimi.it*

Keywords: concrete; anisotropy; damage model; alkali-aggregate reaction.

SUMMARY. Chemical reactions, supported by temperature variations, may produce growing damage in existing concrete structures. With specific reference to the expanding gel produced by the alkali-aggregate-reaction, occurring in many ageing concrete structures such as concrete dams and reinforced concrete bridges, an anisotropic bi-phase coupled chemo-thermo-mechanical anisotropic damage model is proposed, capable to account for the macroscopic strength and stiffness deterioration in the concrete skeleton due to the expanding gel. The model is validated against experimental tests taken from the literature.

1 INTRODUCTION

Deterioration of the mechanical properties of concrete, such as strength and stiffness, can occur in existing structures as the result of severe loading conditions and/or of chemo-physical processes activated by particular environmental conditions. Examples of this type of damages are the deformation and the fracture of porous solids from drying-induced internal crystallization of salt, due to the deposition of saline solutions in the form of salt-spray, and their further penetration by capillary action in the porous structure of the material [1], and the Alkali-Aggregate Reaction (AAR, or alkali-silica reaction, ASR), i.e. the chemical reaction which occurs in concrete between the alkaline cement paste and the non-crystalline silicon di-oxide, often present in aggregates. The main product of the reaction between alkali and silica is a gel, expanding in the presence of water and thereby producing extensive cracking within the concrete matrix. The latter phenomenon is particularly frequent in existing concrete structures such as dams, reinforced concrete bridges, etc., built some decades ago, where the alkali-aggregate reaction is producing swelling phenomena. Deterioration of mechanical properties is observed under the combined action of the internal self-stresses due to the gel expansion and the macroscopic self-stresses due to the structural redundancy which prevents the free expansion of the structure.

Based on the work by Ulm et alii [2], [3], a two-phase isotropic damage model has been recently proposed for the simulation of the swelling phenomena and of the consequent deterioration of local stiffness and strength [4]. Concrete affected by AAR has been conceived, according to Biot's theory of saturated porous media, as a heterogeneous material at the meso-scale, constituted by two elastic-damageable phases: the gel produced by the chemical reaction, and the homogenized concrete matrix. The gel phase exhibits a volumetric expansion in time, promoted by the chemical reaction and supported by increasing temperature, and self-equilibrated stresses at the meso-scale are generated also in the absence of external loading. Under the hypothesis of full saturation, the evolution in time of such expansion is described by a scalar variable, the so called "chemical reaction extent", and depends locally only on the temperature history [2]. The response of the homogenized concrete matrix to the effective stresses has been described by a suitably adapted version of a "bi-dissipative"damage model for concrete, with two isotropic damage variables, one in tension and the other in compression [5].

Within the same framework of two-phase Biot's theory, in the present paper a model is developed for concrete, whereby the anisotropy induced by the evolving damage is explicitly taken into account. Before the beginning of the gel expansion, the behavior of the uncracked concrete is assumed to be isotropic. Initial anisotropy, frequently due to the particular casting procedure adopted, can however be accounted for by assuming an initial directional damage. Under the application of permanent external loads, the microscopic deformation due to the expanding gel in the skeleton pores may become highly anisotropic, producing directional damage which destroys the initially isotropic material microstructure. In the proposed model, damage is described by a single second order symmetric tensor damage variable $\mathbf{D}$, as in [6], leading to an orthotropic behavior at the macroscale, evolving with damage. A free energy potential is formulated in terms of macroscopic strains, tensor damage and chemical reaction extent. Unlike in the isotropic case, the potential contains a damage dependent volumetric-deviatoric coupled term which does not appear in the initial undamaged isotropic state. In the strain space, the elastic domain is assumed to be bounded by a damage activation function evolving with a combination of the principal components of damage. In view of the orthotropy of the damaged stress-strain relation, the resulting elastic domain in stress-space turns out to be affected by the direction of damage growth.

The proposed model has been validated on the basis of experimental data provided by accelerated laboratory tests documented in the literature [7], [8]. These tests, carried out at constant temperature and humidity on cylinders of reactive concrete, under free expansion conditions or with confinement provided by steel rings and different axial loads, allow to check the model prediction in different stress state conditions, evidencing the macroscopic anisotropy of the swelling phenomenon.

2 ANISOTROPIC TWO-PHASE DAMAGE MODEL

2.1 *Mathematical formulation*

The free energy density for the proposed anisotropic model is assumed in the form

$$\begin{aligned}\Psi &= \frac{1}{2}\left[2\mu\boldsymbol{\varepsilon}:\boldsymbol{\varepsilon}+\lambda\mathrm{tr}^2\boldsymbol{\varepsilon}+2\alpha\mathrm{tr}\boldsymbol{\varepsilon}(\boldsymbol{\varepsilon}:\mathbf{D})\right.\\ &+ \left. 4\beta\mathrm{tr}(\boldsymbol{\varepsilon}\cdot\mathbf{D}\cdot\boldsymbol{\varepsilon})+Mb^2(1-\gamma\frac{\mathrm{tr}\mathbf{D}}{3})\left(\mathrm{tr}\boldsymbol{\varepsilon}-\frac{\varepsilon_\infty}{Bb}\xi\right)^2\right]\\ &+ \frac{1}{2}A_0(1-\xi)^2 \qquad (1)\end{aligned}$$

where $\boldsymbol{\varepsilon}$ is the strain tensor, λ and μ are the Lamé's constants, M is the Biot's modulus, b the Biot's coefficient, B the Skempton coefficient, ε_∞ the asymptotic volumetric expansion for $t\rightarrow\infty$ for an unconstrained material (free expansion), $\xi\in[0,1]$ is the chemical reaction extent and A_0 is the initial reaction affinity. $\mathbf{D}$ is the symmetric anisotropic damage tensor defined in terms of its eigenvalues D_k and eigenvectors ν^k as

$$\mathbf{D}=\sum_{k=1}^{3}D_k\nu^k\otimes\nu^k \qquad (2)$$

and α, β are elastic parameters defining the damage induced anisotropic behaviour of the skeleton and γ is a non-dimensional parameter accounting for the gel damage. In the expression (1), the terms depending on the temperature variations have been neglected, for notation simplicity, since the validation tests considered in the present paper have been carried out under isothermal conditions.

The isotropic form of the free energy can be recovered as a special case of (1) when the damage tensor is assumed to be isotropic, $\mathbf{D} = D\mathbf{1}$, with the following choice of parameters: $\alpha = -\frac{\lambda}{2}$, $\beta = -\frac{\mu}{2}$ and $\gamma = 1$.

The stress tensor and the reaction affinity are obtained through the state equations as

$$\boldsymbol{\sigma} = \frac{\partial \Psi}{\partial \boldsymbol{\varepsilon}} = \lambda \mathrm{tr}\boldsymbol{\varepsilon}\mathbf{1} + 2\mu\boldsymbol{\varepsilon} + \alpha[(\boldsymbol{\varepsilon} : \mathbf{D})\mathbf{1} + (\mathrm{tr}\boldsymbol{\varepsilon})\mathbf{D}] + 2\beta[\boldsymbol{\varepsilon}\cdot\mathbf{D} + \mathbf{D}\cdot\boldsymbol{\varepsilon}] - bp\mathbf{1} \quad (3)$$

$$A = -\frac{\partial \Psi}{\partial \xi} = Mb(1 - \gamma\frac{\mathrm{tr}\mathbf{D}}{3})\left(\mathrm{tr}\,\boldsymbol{\varepsilon} - \frac{\epsilon_\infty}{B\,b}\xi\right)\frac{\epsilon_\infty}{B} + A_0\,(1-\xi) \quad (4)$$

where $\mathbf{1}$ denotes the identity tensor and p is the gel pressure defined as:

$$p = -\left(1 - \gamma\frac{\mathrm{tr}\mathbf{D}}{3}\right) Mb\left(\mathrm{tr}\boldsymbol{\varepsilon} - \frac{\varepsilon_\infty}{bB}\right) \quad (5)$$

In equation (5), only the trace of the damage tensor plays a role, assuming in this way that the gel cannot sustain deviatoric stresses. Using this definition of pressure in the definition (4) of the reaction affinity, the latter can be rewritten as

$$A = -\frac{\epsilon_\infty}{B}\,p \,+\, A_0\,(\,1-\xi\,) \quad (6)$$

For the range of pressures of interest in structural applications, the first term in (6) is negligible with respect to the second [2], so that the reaction affinity can be taken as

$$A \simeq A_0\,(1-\xi) \quad (7)$$

The activation of damage is governed by an *inelastic effective stress* $\boldsymbol{\sigma}'' = \boldsymbol{\sigma} + cp\mathbf{1}$ where $c \leq b$ governs the damage level achievable in a concrete specimen under AAR induced free expansion. As in [4], the inelastic effective stress $\boldsymbol{\sigma}''$ is used in the adopted damage activation criterion, which is the one proposed in [5]. Since only tensile damage is activated in the tests used for the model validation, only the expression of f_t is of interest and reads:

$$\begin{aligned} f_t &= 4\mu^2\frac{1}{2}\mathbf{e}:\mathbf{e} \\ &- 9a_t\left[(K + Mb(b-c))\,\mathrm{tr}\boldsymbol{\varepsilon} - (b-c)M\frac{\varepsilon_\infty}{B}\xi\right]^2 \\ &+ 3b_t\left[(K + Mb(b-c))\,\mathrm{tr}\boldsymbol{\varepsilon} - (b-c)M\frac{\varepsilon_\infty}{B}\xi\right]h(\mathbf{D}) \\ &- k_t h(\mathbf{D})^2 \end{aligned} \quad (8)$$

where a_t, b_t and k_t are parameters defining the initial shape of f_t, $K = (3\lambda + 2\mu)/3$ is the bulk modulus and $\mathbf{e}$ is the deviatoric strain tensor. $h(\mathbf{D})$ is a scalar hardening function governing the evolution of the domain in the strain space and is defined as

$$h(\mathbf{D}) = \left[\frac{(1-D_1^d)^{0.75}(1-D_2^d)^{0.75}(1-D_3^d)^{0.75}}{(1-D_1)(1-D_2)(1-D_3)}\right]^{\frac{1}{3}} \quad (9)$$

where the exponent d is a material parameter and D_1, D_2 and D_3 are the principal values of the damage tensor. The damage evolution law is defined as

$$\dot{\mathbf{D}} = \frac{\boldsymbol{\varepsilon}^+}{\mathrm{tr}\boldsymbol{\varepsilon}^+}\dot{\lambda}_t \tag{10}$$

where $\dot{\lambda}_t$ is the rate of a dissipation multiplier to be determined from the Kuhn-Tucker loading-unloading conditions

$$f_t \leq 0; \quad \dot{f}_t \leq 0; \quad \dot{\lambda}_t \geq 0; \quad \dot{f}_t\dot{\lambda}_t = 0; \quad f_t\dot{\lambda}_t = 0 \tag{11}$$

and where $\boldsymbol{\varepsilon}^+$ denotes the positive part of the strain tensor, obtained from the positive part of its principal values by use of the projection tensor $\mathbb{P}^+$

$$\boldsymbol{\varepsilon}^+ = \mathbb{P}^+ : \boldsymbol{\varepsilon}, \quad P^+_{ijkl} = Q^+_{ik}Q^+_{jl} \tag{12}$$

The tensor $\mathbf{Q}^+$ in (12)b is defined as

$$\mathbf{Q}^+ = \sum_{n=1}^{3} H(\varepsilon_n)\mathbf{q}^n \otimes \mathbf{q}^n \tag{13}$$

$\mathbf{q}^n$ being an eigenvector of $\boldsymbol{\varepsilon}$, ε_n the corresponding eigenvalue and $H()$ denoting the Heaviside function, i.e. $H(\varepsilon_n) = 1$ if $\varepsilon_n \geq 0$, $H(\varepsilon_n) = 0$ if $\varepsilon_n < 0$.

2.2 *Physical motivations*

In the model formulated above, developed in the framework of Biot's theory [1], concrete affected by the AAR is conceived as a two-phase material, consisting of the concrete skeleton, obtained from the homogenization of the solid matrix and the interstitial pores, and of the expanding gel. A conceptual representation of the two-phase model is shown in Figure 1 where E_g and E_s denote the elastic moduli of gel and skeleton, respectively. The main assumptions for the model, motivated by physical evidences [9], [7], are: (a) for the typical range of stress states expected in concrete structures, the chemical reaction is independent of the local stress state; (b) the kinetics of the reaction is assumed to depend linearly on the chemical affinity, and nonlinearly on the temperature, according to Arrhenius law (see [9]); (c) the temperature field can be computed a priori since it is not affected by the evolution of the chemical reaction. Moreover, the temperature excursion is limited, so that the mechanical material properties are not affected by temperature changes; (d) the kinetics of the reaction has been shown to depend on the moisture content in the concrete body which is in general not uniform [9]. However, in certain cases, as for instance for massive concrete dams, it can be assumed to be uniform and higher than $90\,\%$ (with the exception of the concrete outer layers) so that the AAR kinetics does not depend on the local level of saturation. The unsaturated case is not considered in the present model; (e) micro-cracking in the concrete matrix can be modelled as a progressive degradation of the elastic moduli and of the peak strength, without significant permanent strains. This is reasonable since the AAR generally produces tensile damage in the skeleton with negligible permanent strains.

Under these assumptions, the development of the chemical reaction can be described through a single scalar variable, the reaction extent $\xi \in [0, 1]$. Its evolution is expressed as

$$\tilde{t}\,\frac{d\,\xi}{d\,t} = 1 - \xi \tag{14}$$

where $\tilde{t}$ is an intrinsic time of the reaction. Larive [9] identified $\tilde{t}$ as a function of the reaction extent ξ and of two time parameters, the latency time τ_{lat} and the characteristic time τ_{ch}, depending on the

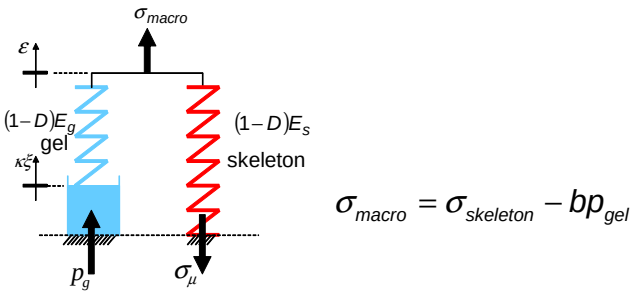

Figure 1: Two phase model

current temperature T [^{o}K] and on the temperature $\overline{T}$ at which the iso-thermal laboratory tests have been conducted, in the form:

$$\tilde{t} = \tau_{ch} \frac{1 + \exp\left[-\tau_{lat}/\tau_{ch}\right]}{\xi + \exp\left[-\tau_{lat}/\tau_{ch}\right]} \tag{15}$$

with

$$\begin{aligned} \tau_{lat}(T) &= \tau_{lat}(\overline{T}) \exp\left[U_{lat} \left(1/T - 1/\overline{T}\right) \right] \\ \tau_{ch}(T) &= \tau_{ch}(\overline{T}) \exp\left[U_{ch} \left(1/T - 1/\overline{T}\right) \right] \end{aligned} \tag{16}$$

Symbols U_{ch} and U_{lat} [^{o}K] denote the Arrhenius activation energies. Typical values of U_{ch} and U_{lat} for the AAR are $U_{ch} = 5{,}400 \pm 500$ ^{o}K and $U_{lat} = 9{,}400 \pm 500$ ^{o}K [2].

3 EXPERIMENTAL VALIDATION AND CALIBRATION

The proposed model has been calibrated and validated on the basis of the experimental tests carried out by Multon, and documented in [7] and [8]. Multon carried out four types of accelerated tests on cylindrical specimens: 1) free expansion tests on unconstrained specimens; 2) expansion tests on unconstrained specimens, subjected to axial compression; 3) expansion tests on specimens confined by steel rings of different thickness; 4) expansion tests on specimens confined as in 3), and subjected to axial compression. The expected expansion due uniquely to the chemical reaction was estimated by subtracting the creep and shrinkage strains (and also the instantaneous elastic effect of loading, if any) from the overall deformation. Multon's tests were carried out on concrete cylinders of 130 mm diameter and 240 mm height, for a duration of 450 days, at a temperature $\overline{T} = 38$ ^{o}C, in order to accelerate the chemical kinetics. A concrete mixture of 0.5 water/cement ratio and a 410 kg/m^3 cement content was used for the preparation of the specimens. The specimens were sealed under a watertight cover, to guarantee a uniform distribution of the moisture content throughout the experiment. The confinement was provided by means of superimposed steel rings, each 10 mm high, with a thickness of 3 and 5 mm. The rings were not connected to each other, so as to leave the specimens free to deform in the axial direction. The steel used had a Young's modulus of 193,000 MPa, and a yield stress of 206 MPa.

The model parameters have been calibrated on the unloaded free expansion test and are summarized in Table 1. The simulation of the free expansion test, shown in Figure 2a, shows a good agreement with both the radial and axial expansions. Since the elastic behaviour (3) is isotropic for the undamaged material, the anisotropic response has been obtained assuming an initial axial damage $D_a = 0.07$.

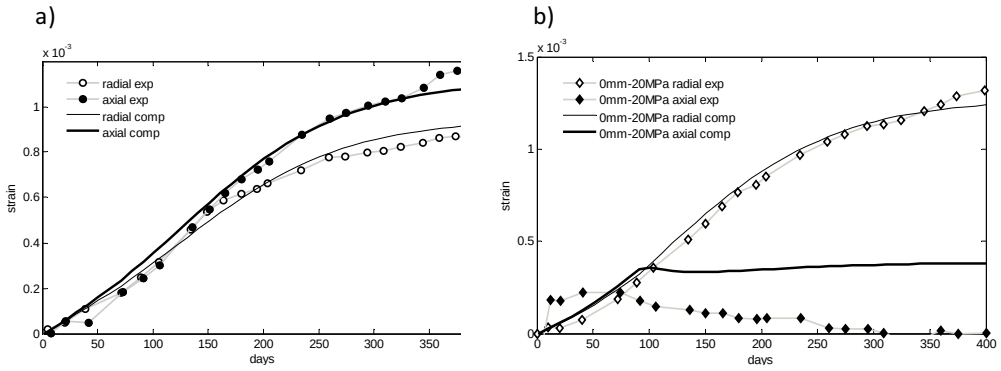

Figure 2: Free expansion tests: experimental time evolution of axial and radial strains, and computed response with anisotropic model. a) unloaded specimen; b) 20 MPa axially loaded specimen.

Table 1: Material Parameters

$\mu = 15287.$ MPa	$c = 0.088$
$\lambda = 12011.$ MPa	$\varepsilon_\infty = 0.0037$
$\begin{pmatrix} E = 37300. \quad \text{MPa} \\ \nu = 0.22 \end{pmatrix}$	$a_t = 0.16$
$b = 0.4$	$b_t = 12.13$ MPa
$M = 6000.$ MPa	$k_t = 51.307$ (MPa)^2
$\alpha = -300.$ MPa	$\tau_{lat} = 126$ days
$\beta = -\frac{\mu}{2} = -7643.$ MPa	$\tau_{ch} = 74$ days
$\gamma = 1.$	$d = 10$

With the same parameters calibrated on the free expansions test, see Table 1, the anisotropic model has been validated on some of the other tests carried out in [7]. Figure 2b shows the results of the simulation of the expansion test under an axial compressive load of 20 MPa. While the radial curve fits very accurately the experimental data, the axial strain overestimates the experimental one, even though the general trend is caught correctly by the model.

The time evolution of the axial and radial damages D_a and D_r is shown in Figure 3 for the free expansion test and for the 20 MPa axially loaded test. It can be appreciated that the axial damage starts from a value different from zero and that the final asymptotic state in free expansion is reached for a relatively low final value of damage, accounting for the residual material strength which can be observed experimentally. For the case of an applied compressive axial load of 20 MPa, damage develops only in the radial direction, correctly reproducing the stress induced damage anisotropy.

In his experimental campaign, Multon [7] also carried out expansion tests on specimens confined by steel rings 3 and 5 mm thick. Figure 4 shows the results of the simulations of these tests. The axial strain is shown in Figure 4a, while the radial strain in Figure 4b. In both cases the physical trend is correctly reproduced by the model: the axial strain increases with increasing confinement stiffness while the radial strain decreases. Under this respect, it should be noted that the experimental result in

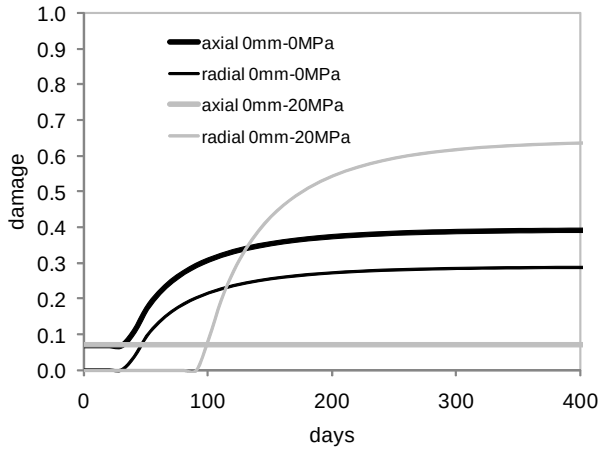

Figure 3: Free expansion tests: time evolution of axial (thick curves) and radial (thin curves) damages for unloaded and axially loaded specimens.

Figure 4b is counterintuitive: the radial expansion is higher with the thicker 5 mm confinement. The authors of the experiments in [7, 8] attribute this counterintuitive experimental result to an improper levelling of the rings which prevented from accurate measurements. This is not the case of the simulation, where the expected trend is obtained. Under the quantitative point of view, the axial strain is reproduced more accurately, also in view of unexpected experimental radial response.

The anisotropic damage growth during the different tests induces a reduction of the Young modulus in the different directions. For the considered tests, Figure 5 shows the polar diagrams of $E(\mathbf{m})$, $\mathbf{m}$ being a unit vector inclined of an angle θ with respect to the axial direction, at the assigned time instants $t = 0, 100, 200, 300, 400, 500$ days. A certain level of damage corresponds to each assigned time and is therefore constant for each polar curve. The dashed circular line corresponds to the undamaged isotropic case and it is shown as a reference in all plots. Due to the assumed initial axial damage, the anisotropic effect is present since the beginning. The polar diagrams effectively show the anisotropic damage evolution and the effects of the vertical load and radial confinement. In particular, from Figure 5b, one can observe that the vertical load on the unconfined specimen, while reducing the Young modulus degradation in the axial directions, severely contributes to a more pronounced degradation of the corresponding modulus in the radial direction. A similar, though less pronounced, effect can be noted from Figure 5e, where the strong lateral confinement in the absence of a vertical load, promotes the degradation of the axial modulus.

4 CONCLUSIONS AND FUTURE WORK

In the present paper an anisotropic chemo-damage model, based on the isotropic version developed in [4], has been proposed for the simulation of the mechanical consequences of the AAR in concrete. The present model has the capability to deal with a possible initial material anisotropy and with the subsequent AAR damage induced anisotropy. The anisotropic model has been used to simulate some of the experimental tests carried out by Multon [7] obtaining good physical correspondence with the experimental evidences. In particular, it has been shown that the initial material anisotropy can be well reproduced by assuming an initial damage in the specimen axial direction.

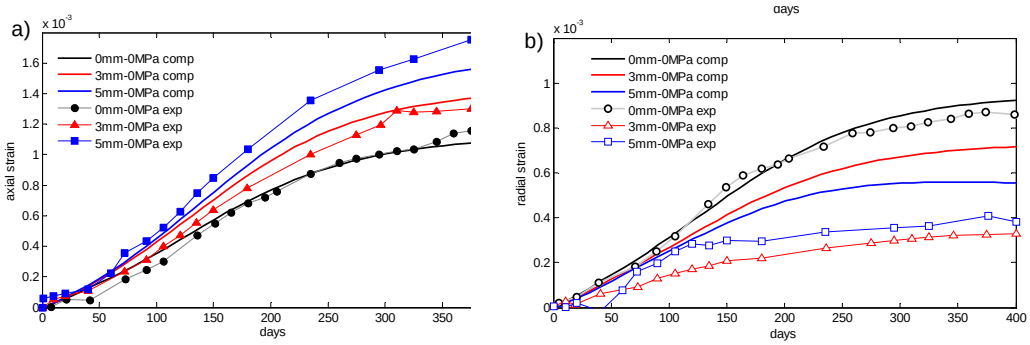

Figure 4: Confined tests: axial (a) and radial (b) strains due to AAR. Experimental (symbols) vs. simulation (curves) results.

Polar diagrams have been used to synthesise the anisotropic evolution of Young's modulus in the different directions.

5 Acknowledgements

The present work has been carried out in the framework of the PRIN_20077ESJAP_001 research project. The financial support of the Italian MIUR is gratefully acknowledged.

References

[1] Olivier Coussy. Deformation and stress from in-pore drying-induced crystallization of salt. *Journal of the Mechanics and Physics of Solids*, 54(8):1517–1547, August 2006.

[2] F.J. Ulm, O. Coussy, L. Kefei, and C. Larive. Thermo-chemo-mechanics of asr expansion in concrete structures. *ASCE Journal of Engineering Mechanics*, 126(3):233–242, 2000.

[3] F.J. Ulm, M. Peterson, and E. Lemarchand. Is ASR-expansion caused by chemo-poroplastic dilatation? *Journal of Concrete Science in Engineering*, 4:47–59, 2002.

[4] C. Comi, R. Fedele, and U. Perego. A chemo-thermo-damage model for the analysis of concrete dams affected by alkali-silica reaction. *Mechanics of Materials*, 41(3):210–230, 2009.

[5] C. Comi and U. Perego. Fracture energy based bi-dissipative damage model for concrete. *International Journal of Solids and Structures*, 38:6427–6454, 2001.

[6] D. Halm and A. Dragon. An anisotropic model of damage and frictional sliding for brittle materials. *European Journal of Mechanics - A/Solids*, 17(3):439–460, 1998.

[7] S. Multon. *Evaluation expérimentale et théorique des effects mechaniques de l'alcali-réaction sur des structures modéles*. PhD Thesis, LCPC, 2003.

[8] S. Multon and F. Toutlemonde. Effect of applied stresses on alkali-silica reaction-induced expansions. *Cement and Concrete Research*, 36:912–920, 2006.

[9] C. Larive. *Apports combinés de l'expérimentation et de la modélisation la comprehénsion de l'alcali-réaction et de ses effets mécaniques*. PhD Thesis, LCPC, 1998.

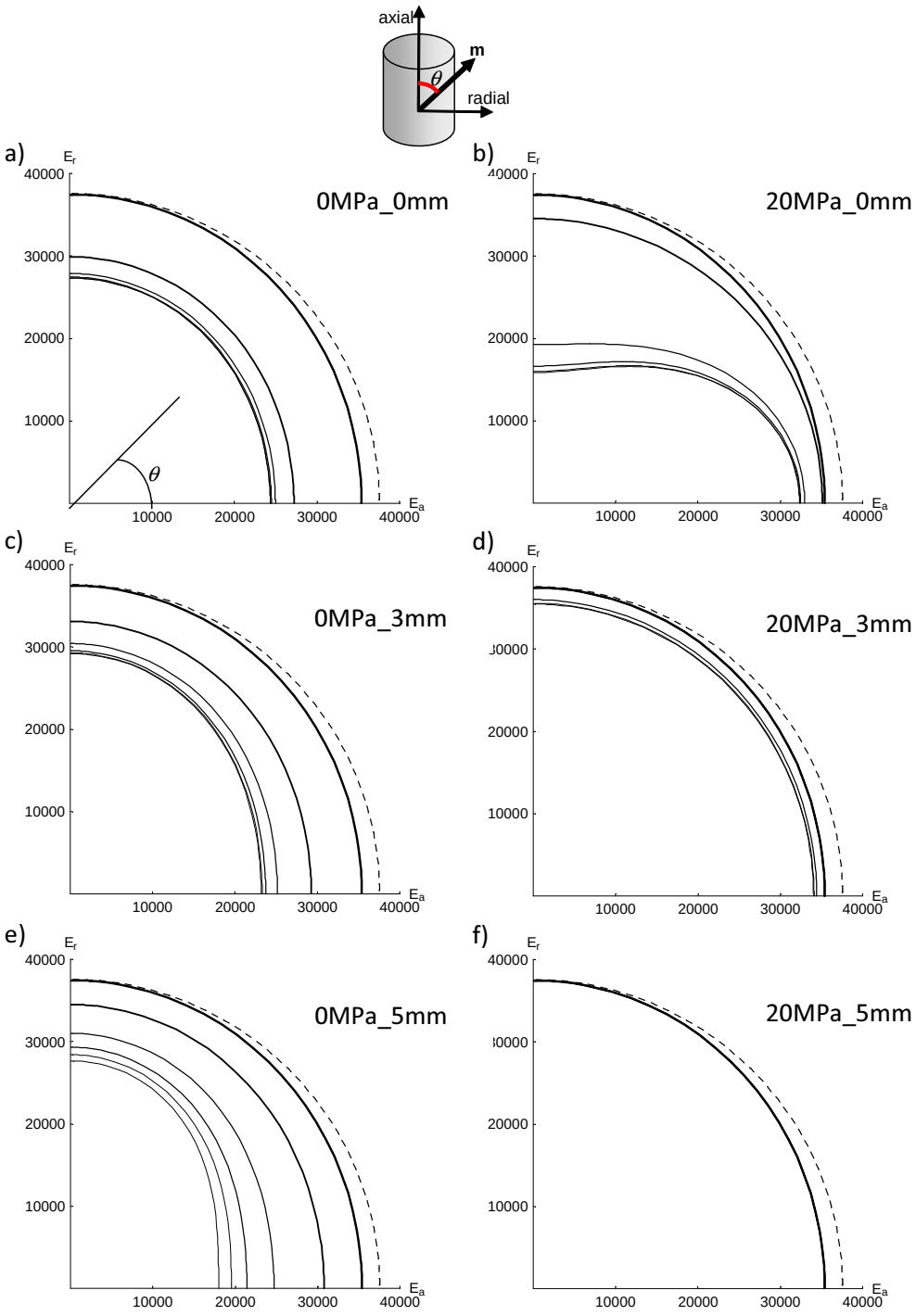

Figure 5: Multon's tests. Polar diagrams of elastic moduli.